COTS Lens and Detector Characterization for Low Cost, Miniature SAL Seekers

Randal Allen[1], John Volpi[2], and Steve Roemerman[3]
Lone Star Aerospace, Addison, TX, 75001

In the spirit of lower cost, weight, and volume, a simple aspheric refractor lens is characterized with a square detector for Semi-Active Laser (SAL) seeker applications. Experimental results show an angular error of 0.176 degree over an angular range of ±6 degrees (linear region of the detector) and an error of 0.097 degree over a range of ±4 degrees. In the final 10 seconds of a typical end-game SAL engagement, the slant range is approximately 2500m, corresponding to a target location error of 7.7m in the former case and 4.2m in the latter case. These initial results are very encouraging as the experimental research continues by replacing the square detector with a quad cell detector.

I. Introduction

OVER roughly five decades since SAL guidance was first deployed, seekers have become more complex, but system-level accuracy has not improved much. This is partly due to the attitude that it was good enough already. Additionally, some second generation requirements were implemented with 1970's or 1980's technology and have not been revisited since. A lack of interdisciplinary systems integration has partitioned requirements in ways that has added cost and risk in some cases.

More recently, SAL guidance has been adopted for higher dynamic systems with legitimately more demanding requirements. In some cases these applications have added costs, with little or no system-level performance improvements. Two specific examples of needed performance improvement are angular accuracy of sufficient precision to support estimate of line-of-sight rate for guidance schemes more sophisticated than early pursuit approaches and small tube-launched systems such as guided mortars. SAL seekers represent technology that has gone from analog to digital without orders-of-magnitude improvements in value.

These considerations explain why seekers exhibit significant complexity, e.g. 2 to 3 gimbals and 3 to 10 optical elements. Of course, complexity increases when more than one seeker mode is used (e.g. IR and SAL for a dual mode seeker) and with that complexity comes still higher cost, higher component count, and lower reliability.

For SAL applications in particular, the seeker attributes are somewhat dated due to a continuation of past design compromises, e.g. the use of parabolic optical objectives; limited hardware/software integration, e.g. Hellfire has Electronic Counter-Countermeasures (ECCM) in a separate chip and Paveway III has gyros on its gimbals as well as body-fixed gyros; and functional separation, e.g. sensor stabilization is generally separate from the Line-of-Sight (LOS) estimator and error correction (if any) is performed by additional optical elements.

Early seekers were large and expensive, but this was acceptable because they were only used for very high-value missions. Mechanical and electronic guidance subsystems were large, but seeker volume and weight did not matter much; warheads were also large, usually 1,000 kg or more; and the cost of other system components were large, so seeker costs, though not insignificant, were tolerated.

Today, guided weapons are generally smaller and far less expensive. Other components (e.g. signal processing, warheads, and actuators) are orders of magnitude smaller and the trend is toward lower cost, weight, and volume. Table 1 compares previous seeker attributes with what is currently desired.

---

[1] AIAA Associate Fellow
[2] Vice President and CTO
[3] President and CEO

Table 1 Comparison of Seeker Attributes

Seeker Attributes	Previous	Desired
Volume (cm^3)	> 10,000	< 100
Weight (kg)	> 50	< 1
Outer moldline	Seeker-defined	Airframe-defined
Guidance loops	Simple, linear, analog	Complex, non-linear, discrete
Countermeasure (CM) resistance	Limited	Robust
Flight time (sec)	> 60	< 10
Accuracy re: collateral damage	Limited	Critical
Performance vs cost	Performance more important than cost	Cost more important than performance

By utilizing technology currently available to the designer, and by taking a systems approach to the seeker as part of larger guidance architecture, this study shows small, low-cost Commercial-Off-The-Shelf (COTS) components may be used to replace larger and more expensive components for the SAL seeker system.

What follows is an overall description of the procedure used for testing and employing this class of components, a presentation of the results with the corresponding discussion, and conclusions and future (current) work being conducted to further this, patents pending, design approach.

II. Procedure

Figure 1 shows a block diagram of the test equipment used in the experiment.

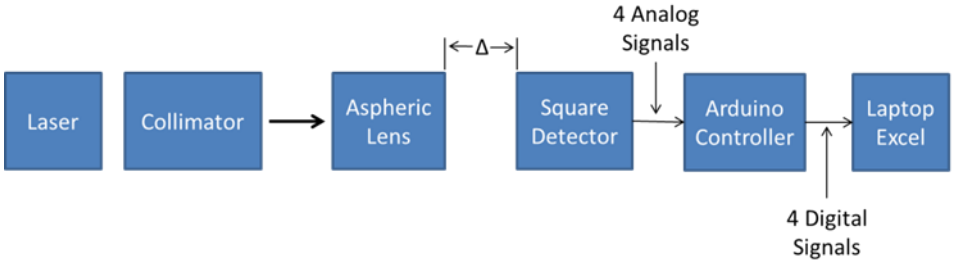

Figure 1 Block diagram of test equipment

The major elements of the test equipment consist of a laser and collimator, a lens and square detector, and a microcontroller and PC laptop. The variable spacing (Δ) between the lens and the square detector is to investigate the effect of defocusing. All of the optical elements are mounted on a 4'x6' optical bench. A discussion of each element follows.

The collimator focuses the laser to a 1" diameter spot so that the Edmund 27mm X 13FL aspheric lens receives parallel rays. The aspheric lens corrects for spherical and comatic aberrations. There is no chromatic aberration because the laser is coherent. The lens is mounted to a Zaber motion controller with rotational increments of 4.0906 microrad. An Arduino MEGA 8-bit microcontroller is used to control the overall test, including the Zaber motion controller. As mentioned previously, the variable spacing (Δ) between the lens and the square detector is to investigate the effect of defocusing.

The Pacific Silicon (First Sensor) square detector is a 20mm X 20mm dual-axis position-sensing diode on a printed circuit board with sum and difference amplifiers. The 4 analog outputs are described below:

- X: The X output is proportional to the X-centroid of the light impinging on the detector.
- Y: The Y output is proportional to the Y-centroid of the light impinging on the detector.
- XSUM: The (negative) sum of all the light in the X-direction, which is used for normalizing.
- YSUM: The sum of all the light in the Y-direction, which is used for normalizing.

By normalizing the X and Y signals with the algorithms X/(-XSUM) and Y/YSUM, the signals become independent of fluctuations in light spot intensity.

Figure 2 shows the major elements of the test equipment in the laboratory, including the laser and collimator, the elevation and azimuth rotations and the vernier for lens/detector spacing, and where the Wratten filters are located.

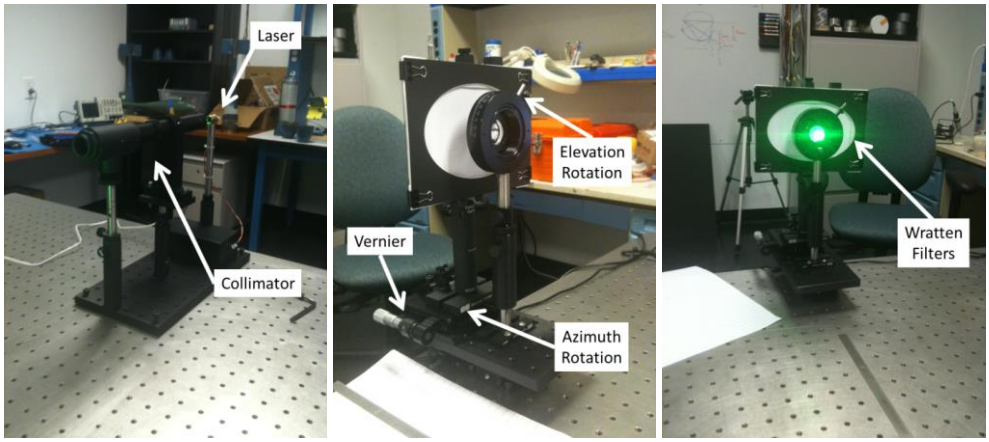

Figure 2 Left: laser/collimator, center: azimuth/elevation rotations, vernier, right: Wratten filters

The experimental data collection steps are outlined below:

- Step 1: Manually rotate the lens about the optical axis to -90 degrees (elevation angle)
- Step 2: Set the azimuth angle of the Zaber to bore sight minus 30 degrees
- Step 3: Turn the laser on for 2 seconds, take 5 readings at 500 millisecond intervals, turn the laser off, filter the data and write it to an Excel spreadsheet
- Step 4: Increment the azimuth angle by 1 degree
- Step 5: Repeat steps 3 and 4 until the azimuth is bore sight plus 30 degrees
- Step 6: Rotate the lens about the optical axis in 15 degree increments (elevation angle)
- Step 7: Save the Excel data
- Step 8: Repeat steps 2 through 7 until the lens has been rotated to +90 degrees
- Step 9: For each complete set of elevation/azimuth data, vary the spacing between the lens and the detector from the focal plane, to 9mm in front of the focal plane, in 3mm increments. This is to assess the effect of defocusing the laser spot.

Figure 3 illustrates the classic laser "quad cell" detector and shows two spots, one small/focused and one large/defocused. For this simple example, we ignore dark current and limiting factors, and assume the total number of photons is the same in each spot. If the laser spot is defocused such that some of the energy spreads into quadrant I (Figure 3, right), then only a relatively small control signal down and slightly right would be needed to center the laser spot, which results in less demand on the control system. On the other hand, if the laser spot is too small (Figure 3, left), it could be anywhere in quadrant II, relative to bore sight – thus requiring a relatively large control signal down and to the right to center the laser spot.

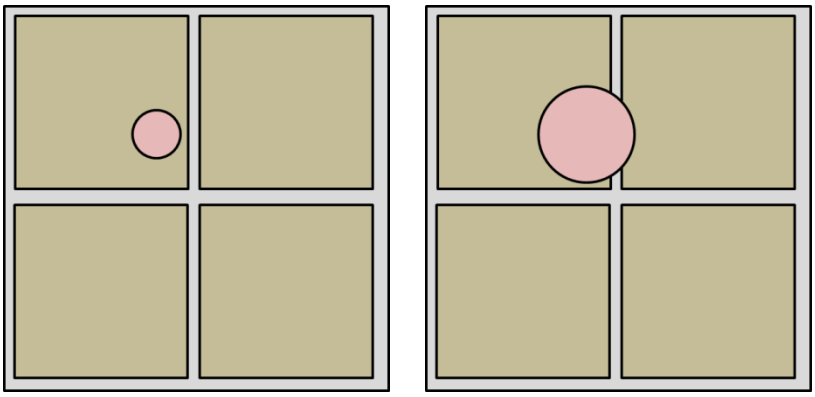

Figure 3 Comparing defocused laser spots

The large defocused spot is a traditional means to implement a seeker intended for pursuit guidance, and was commonly used in first generation systems with "bang-bang" actuator systems. This experiment seeks to explore the performance of such a simple design with modern signal processing instead of expensive hardware components. A commonly held view among seeker designers has been to believe it was not possible to have a large region of

linear angular response (needed for schemes more advanced than simple pursuit guidance) unless there was a large, complex optical system. We sought to challenge that assumption.

For ease of system check out, the initial experiments are conducted with a visible green laser. In order to avoid saturation of the sensor by the 50mW green laser, Wratten filters are used to reduce the power. This is done systematically, measuring the 4 analog outputs of the square detector. For this application, 10%, 50%, and 80% filters are used to produce a transmittance of 4% or 2mW that does not produce sensor saturation. Calibration factors are obtained by working through the mathematics of the Arduino's 5V/10-bit Analog-to-Digital Converter (ADC) and the electronic circuitry (scale factor and bias).

After data is collected from the green laser, it is replaced with a 30mW IR laser. For this application, 10%, 50%, and 50% filters are used to produce a transmittance of 2.5% or 0.75mW that does not produce saturation. Again, calibration factors are obtained by working through the mathematics.

III. Results and Discussion

A. Visible (green) Laser Data Analysis

The first set of raw data plotted for analysis is shown in Figure 4. Each of the four plots shows an elevation/azimuth data point (red) compared with the true elevation/azimuth line (black), in angular increments of 15 degrees. As the spacing between the lens and detector is increased (0mm to 9mm), the defocusing causes some of the laser energy to be spread into the upper and lower halves of the detector at the edges of the azimuth range, i.e. bore sight minus 15 degrees and bore sight plus 15 degrees. The COTS lens is axially-symmetric with regard to manufacturing.

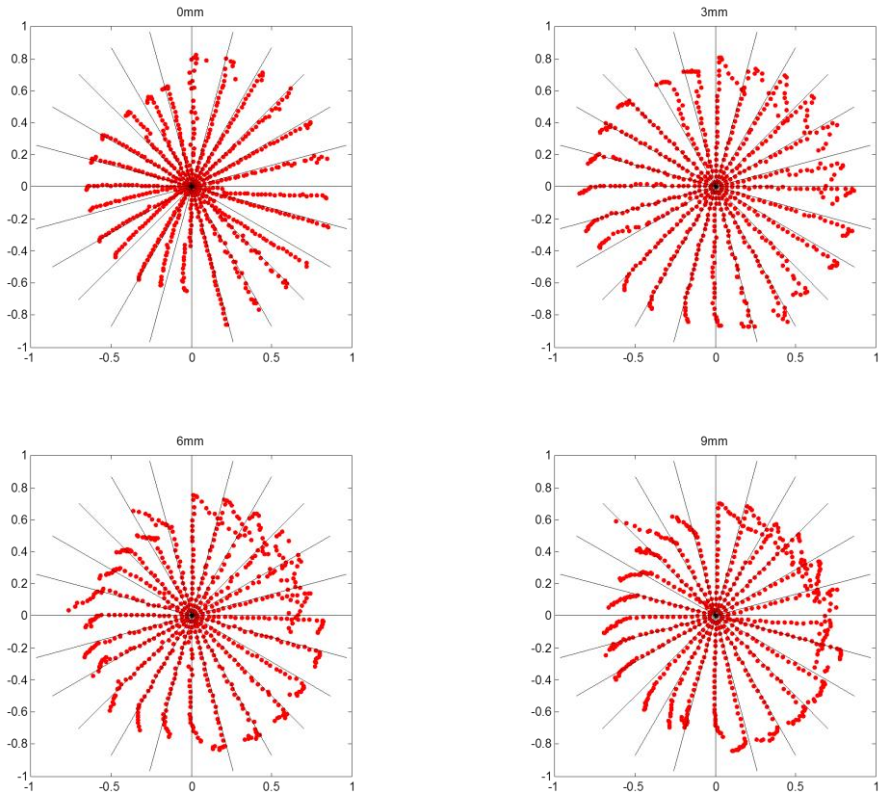

Figure 4 Effects of defocusing, represented by azimuth/elevation (top left: 0mm, top right: 3mm, bottom left: 6mm, bottom right: 9mm)

The next set of raw data plotted for analysis is shown in Figure 5. Each of the four plots shows the azimuth error over the range of azimuth (±30 degrees) for the lens/detector spacing (0mm to 9mm). As the green laser spot is defocused, saturation increases at the tails and the linear region is shortened. For the focal plane (0mm) and the

3mm defocused laser spot, the linear region is approximately ±25 degrees. At 6mm, the linear region is reduced to ±20 degrees. Finally, at 9mm, the linear region is approximately ±15 degrees. While a defocused laser spot is desirable, continual defocusing reduces the linear region of the detector.

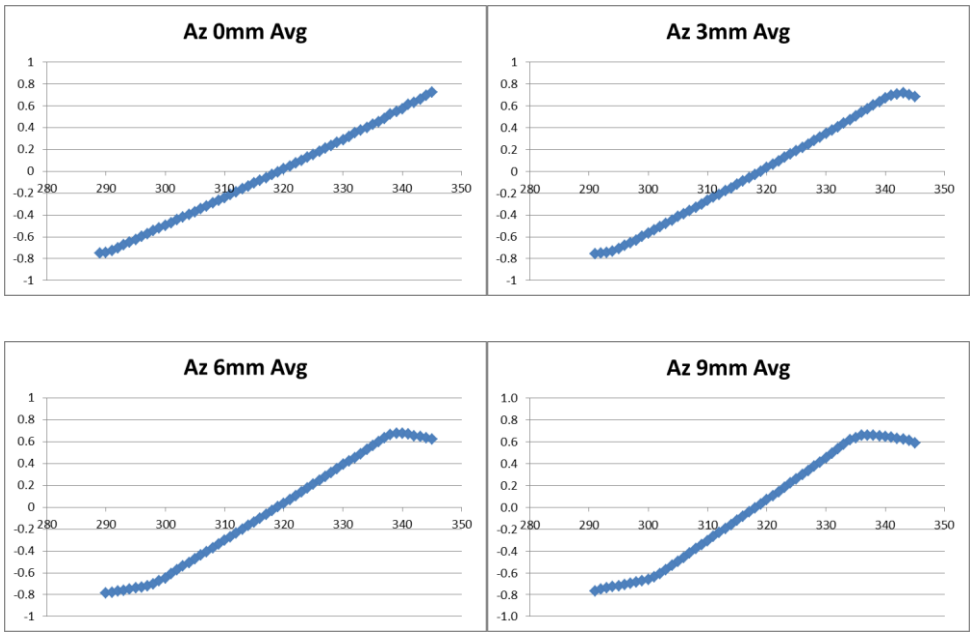

Figure 5 Azimuth error for visible (green) laser

B. IR Laser Data Analysis

In this section, the data plotted for analysis in Figure 6 is obtained by switching the source from the visible green to the IR laser. Each of the two plots shows the azimuth error over the range of azimuth (±30 degrees) for the lens/detector spacing (0mm and 3mm). As the IR laser spot is defocused, the saturation occurring at one end becomes more apparent. For both of these plots, the linear region is approximately ±25 degrees. Here, the implication is that the maximum linear region is still ±25 degrees – as it is for the visible (green) laser.

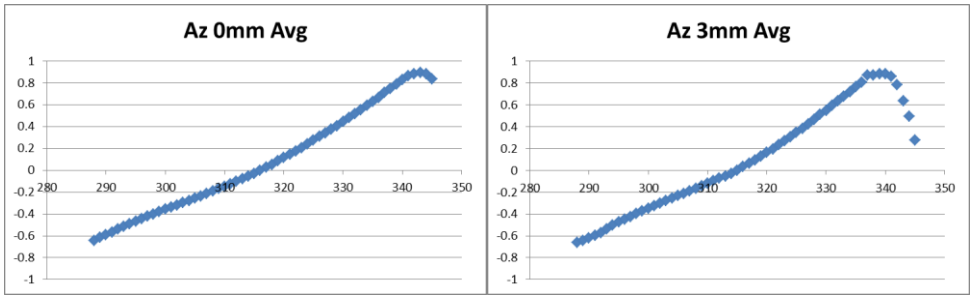

Figure 6 Azimuth error for IR laser

The results of the previous sections direct the detailed analysis of azimuth errors for the IR laser associated with the 3mm defocused data. Figure 7 shows two sets of points, linearly fitted for an azimuth range of ±6 and ±4 degrees, respectively.

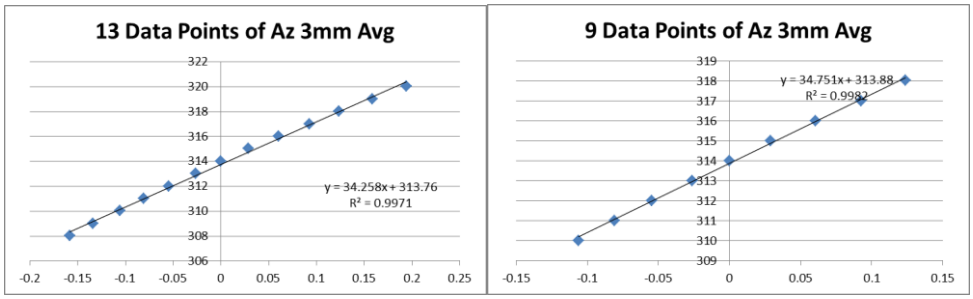

Figure 7 Linear curve fits for ±6 and ±4 degrees of azimuth

Using the fitted data to compute the azimuth angle and the error in azimuth yields the results in Table 2.

Table 2 Azimuth error

Azimuth Range (degrees)	Azimuth Error (degrees)
±6	0.061
±4	0.039

By using a COTS lens/square detector, accurate angular sensing is achieved over a linear region of the detector which is useful in many guidance applications.

C. Error Sources

At this time, it is worthwhile to mention some of the error sources associated with this experiment – all of which will be minimized in on-going experimental research. Optical systems are very sensitive to alignment. When the visible laser is mounted, it is aligned (by eye) for height and yaw. For example, when the thumb screw is tightened, there is a moment on the vertical shaft causing a misalignment in pitch as well. These misalignments are exacerbated when working with the IR laser. Additional (height and yaw) errors are associated with the visual alignment of the collimator and the lens. Finally, the detector has errors in height and yaw, with the addition of cross-plane misalignments. Ideally, the laser spot is centered on the detector. These errors have been identified, a mechanical system has been designed to minimize these misalignments, and will be used in continuing research mentioned in the next section.

IV. Conclusions

This experimental research shows that a COTS lens and square detector make the production of a low-cost, light-weight, small-volume SAL seeker feasible. With proper (and patent pending) signal processing to correct the errors, the resulting information supports nearly any type of guidance law.

There are several reasons "why" these results, which may seem surprising, were the outcome of our work. Since the lens is aspheric, there is no spherical or comatic aberration, and because the laser is coherent, there is no chromatic aberration. Data taken with the visible (green) laser shows the manufacturing process of the lens is radially symmetric, and a reasonable spacing for defocusing the laser spot, using this particular lens, is 3mm in front of the focal plane – which provides the maximum angular range for the linear region of the detector.

Finally, data taken with the IR laser shows an angular error of 0.176 degree over an angular range of ±6 degrees and an error of 0.097 degree over a range of ±4 degrees. In the final 10 seconds of a typical end-game SAL engagement, the slant range is approximately 2500m, corresponding to a target location error of 7.7m in the former case and 4.2m in the latter case. These results challenge high performance and expensive seekers in production today.

V. Future Work

Ongoing research is replacing the square detector with a quad cell detector. After calibration, initial data taken with the IR laser saturates within only a few degrees of azimuth range. This saturation is coming from the current analog amplifiers which should be replaced with log amps. Therefore, before data is collected again, recalibration is necessary. Additional areas of research forthcoming (but not included here) are sensitivity, pulse characteristics, dynamic range, and optical filtering bandwidth.

References

Salles, L., and de Lima Monteiro, D., "Designing the Response of an Optical Quad-Cell as Position-Sensitive Detector" *IEEE Sensors Journal*, Vol. 10, No. 2, 2010.

McManamon, P., Watson, E., and Eismann, M., "Suggestions for Low Cost Multifunction Sensing" *IEEE Aerospace Conference*, Vol. 1, pp. 283-307.

Dubner, H., "Optical Design for Infrared Missile-Seekers" *Proceedings of the IRE*, Paper 4.2.2, 1959, pp. 1537-1539.

Eichblatt, E., *Test and Evaluation of the Tactical Missile*, Progress in Astronautics and Aeronautics, Vol. 119, AIAA, 1989.

Hovanessian, S., *Introduction to Sensor Systems*, Artech House, 1988.

Zissis, G., *The Infrared & Electro-Optical Systems Handbook*, Infrared Information Analysis Center and SPIE Optical Engineering Press, 1993.

Hect, E., *Optics*, Addison Wesley, 2nd ed, 1987.